

Moving breathers in a chain of magnetic pendulums

F. M. Russell, Y. Zolotaryuk, and J. C. Eilbeck

Department of Mathematics, Heriot-Watt University, Edinburgh EH14 4AS, United Kingdom

T. Dauxois

Laboratoire de Physique, Ecole Normale Supérieure de Lyon, 46 Allée d'Italie, 69364 Lyon Cedex 07, France

(Received 26 July 1996)

We describe an experimental model consisting of an anharmonic chain of magnetic pendulums acting under gravity. This is a simple paradigm for the study of *moving breathers* in a discrete system. These highly mobile and strongly localized *dynamically stable* oscillating states are observed experimentally and studied both analytically and numerically. [S0163-1829(97)03810-1]

I. INTRODUCTION

Nonlinear localized excitations with internal oscillations, called breathers, have been exhibited in a number of model nonlinear systems. Unlike the more studied topological solitons, breathers need no activation energy for their creation and this circumstance explains their importance for bridging the gap between the highly nonlinear topological modes (very stable) and the linear phonon modes easily excited by thermal excitations. Generally, in nonintegrable systems it is known that localized *stationary* breather modes do not exist in the continuum limit and the discreteness is an important feature for explaining their existence and stability.^{1,2} However few exact results are known for *moving* breathers which form the main subject of this paper.

There is sometimes some confusion between the word “soliton” and “breather,” so a few words of explanation may be in order. Single solitons take the form of a single bell-shaped or tanh-shaped pulse in one of the field variables. Stationary breathers normally take the form of a bell-shaped pulse whose amplitude is a periodic function of time. Moving breathers are a nonlinear version of the well-known linear wave packet, with the *envelope* of the “carrier” wave having a bell shape. Thus a moving breather is often referred to as an envelope soliton. In some studies such as the nonlinear Schrödinger equation, the practice has been to drop the “envelope” part of the name and refer to modulated pulses simply as “solitons” where “breathers” would be more correct. A strongly localized moving breather (such as the ones discussed in this paper) will have only one or two wavelengths of the carrier wave within the half width of the envelope.

Recent studies of nonlinear localized excitations in homogeneous³ lattices (or with impurities⁴) have attracted interest to these breather modes. In addition to the important discovery of the effect of discreteness, such excitations have become very important in the last few years because of a new mechanism of growth: it has been shown that in nonlinear lattices the collision of such localized excitations could give rise to localization of energy⁵⁻⁷ and therefore such large-amplitude excitations could be found in real systems despite nonzero friction.

We should stress that although breather modes have been

heavily studied in numerical simulations of nonlinear lattice models, there is no way of observing them directly in atomic systems, so the evidence for their existence is indirect. This paper contains a detailed account of the observation and experimental study of breathers; their existence in discrete sine-Gordon (SG) models has been known for some time.⁸

Our motivation in this study is the possibility that moving breathers are important for describing the transfer of energy from atoms or ions moving at relatively high speed to atoms in a solid or crystal with which they collide. This interest arose from the discovery of tracks in doped muscovite mica crystals that could be understood in terms of the breather modes.⁹ These tracks occurred under meta-stable conditions induced by supercooling when perturbations of the lattice could trigger irreversible phase transitions.¹⁰ Effectively mica acts as a 300 million year old particle detector, in many cases a more cost-effective system for study than more modern detectors.

The transfer of energy from highly energetic atoms or ions to a crystal underlies many processes, often of industrial importance. Although usually occurring at a surface, as on blades in a gas turbine or on a space vehicle shield, it can also occur within the bulk material, as with neutrons in a nuclear reactor. As a result, the atoms in a solid gain energy with consequent rise in the bulk temperature, which can be understood in terms of phonons. However, there is a gap in detailed understanding of the energy processes coupling the energetic incident particles, with energies in the range 1 to 100 eV or more, to phonons with energies of 0.01 eV or less. This also spans the chemical binding energy range. Difficulties arise from the nonlinear nature of the particle interactions. The initial interaction between an energetic atom or ion and the lattice is essentially a two-body collisional problem but the subsequent transient behavior of the lattice is a many body problem with its attendant difficulties of analysis. Moreover, all the interactions involve nonlinear forces and this fact suggests that the equations for energy transport might have solitonlike or breatherlike solutions.

In collisional processes the conservation of energy and momentum suggests some type of solitons/breathers might be produced. However, until the mica study, there was no direct evidence for their existence between the point of their

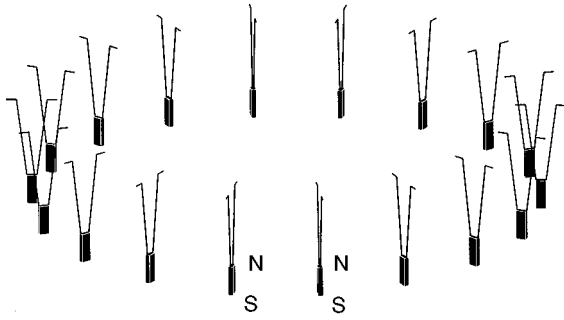


FIG. 1. A circular chain of magnetic pendulums.

supposed creation and final demise. Detection in flight is nontrivial as solitons/breathers are uncharged and propagate with little or no loss of energy.

II. COUPLED MAGNETIC PENDULUMS

To study the conditions leading to the tracks in mica, molecular dynamics methods were used to determine interparticle forces as a function of position in the lattice. It was found that the tracks were associated with particular crystal-line directions in the lattice. The mechanism for selecting these particular one-dimensional (1D) motions in a two-dimensional crystal has been studied in hard sphere models.¹¹

In the preferred directions, the nonlinearity of potential is expressed as $\Psi(r) = \alpha r^2 + \beta r^3 + \delta r^4$, where $\alpha = 0.8 \text{ eV/\AA}^2$, $\beta = 0.38 \text{ eV/\AA}^3$, and $\delta = 0.14 \text{ eV/\AA}^4$ (see Refs. 9 and 12). It is this one-dimensional motion we concentrate on in the present paper.

To study the dynamical behavior in these preferred directions, an analogue model of magnetic pendulums was constructed with similar nonlinearity of force as in the muscovite system. The model consists of eighteen short dipole magnets freely suspended by rigid struts from pivots spaced at equal intervals to form a linear chain. In this model the struts provide a centralizing restraint analogous to the influence of the surrounding lattice which constrains atoms moving along the chain from one unit cell to the next. The gravitational potential mimics the onsite potential in the mica caused by layers above and below the 2D potassium sheets. The dipole-dipole interactions between the magnetic pendulums approximates in some way the atomic forces between the K atoms.

Experiments with this model showed that large impulses rapidly evolved to breatherlike solitons but reflections from the ends rapidly degraded the signal. To overcome this problem, a second model was constructed also with eighteen magnets but arranged in a circle (see Fig. 1), so that perturbations could propagate around the circular chain unimpeded by ends. To initiate a disturbance, one magnet was held fixed and an impulse was given to the next magnet, the fixed magnet being released before the propagating disturbance reached it. The response of the model to various starting conditions was recorded by sequential flash photographs (taken from above the circular chain) from which instantaneous displacement of the magnets from their equilibrium positions could be approximately determined.

We stress that this model and the results we report here

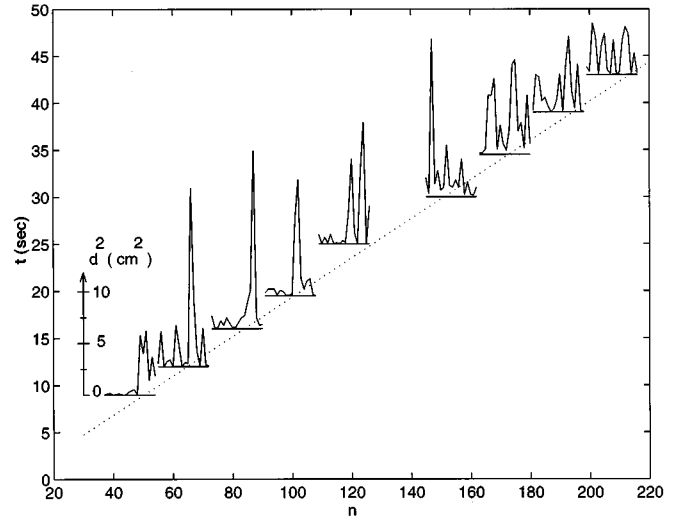


FIG. 2. The experimental observation of the breather propagation in the chain of magnetic pendulums with the initial excitation $\theta_2(0) \approx 0.1$ and the spacing $a = 4.0 \text{ cm}$.

are relatively crude (the model was constructed in the first author's garage without any technical or financial support). For example, there is a fair bit of friction at the pivots, and the need to go to a circular system to avoid boundary effects has not been properly modeled in the numerical study. Nevertheless the reasonable overall agreement between theory and experiment is encouraging, and we hope to produce a more accurate and detailed study when circumstances allow.

The general behavior of impulses in the model strongly suggested resonant coupling between adjacent particles in the lattice leading to nearly antiphase motions. Small impulses spread at a constant speed, the resulting oscillations having maximum amplitude near the impulse site. Large impulses rapidly evolved into compact wave packets concentrated over a small number of sites which propagated freely over many lattice sites before becoming degraded (see Fig. 2). It is these objects that we term breathers. Since the breather traversed the ring several times between photographs, in plotting Fig. 2 we represent the circular chain by its linear analog, ignoring the complication that the low-amplitude "radiation" will propagate round the ring and interfere with the primary pulse. This effect eventually leads to degradation of the primary pulse as shown in the figure at larger times. In order to emphasize the breather against the linear background modes we have plotted the *square* of the horizontal component of the displacement $d_n = l \sin \theta_n$ of each pendulum in Fig. 2. Here l is the pendulum length and θ_n is the angular deviation of each pendulum. The average velocity $v = 4.83 \text{ sites/sec}$ is represented on the plot by a dotted line.

Despite many attempts it was found to be virtually impossible to generate any other type of disturbance, in particular, a Toda-like soliton. Further study showed that the internal structure of breathers moves with a phase velocity much greater than the group velocity.

Experiments explored the evolution of breathers from simultaneous impulses to several adjacent particles in the chain and from multiple impulses to the first particle. The

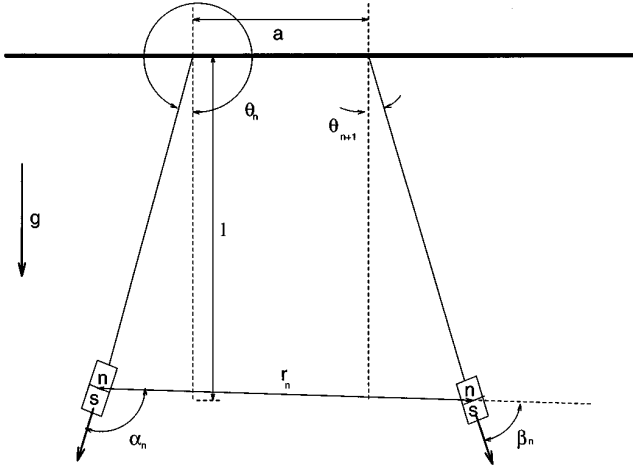


FIG. 3. The schematic representation of the model of interacting magnetic pendulums.

model also demonstrated the stability of breathers against small random defects or perturbations. Other experiments with this model demonstrated the creation of oppositely directed pairs of breathers within the chain and the creation of stationary breathers, the survival of oppositely directed breathers after their mutual interactions, their reflection from boundaries and discontinuities. Much of this behavior is characteristic of integrable systems, but it is emphasized here that these breathers will almost certainly not satisfy exact solitonic conditions in connection with their long-term structural and lateral stability or in their collisional properties.

Such physical models are very instructive but they cannot easily yield quantitative results. Hence, it is difficult to explore in detail the behavior for different impulse strengths and for long propagation paths. To make further studies of breather behavior in this mechanical model, it is necessary to use analytical and numerical methods.

III. THEORETICAL MODEL

Now we develop the dynamical theory of this model. As shown in Fig. 3 (the magnets move in the plane, tangential to the circular backbone), the chain parameters are the spacing a , the pendulum length l , mass M , and the magnetic moment $\mathbf{m} = \mu \mu_0 \phi I d \mathbf{l}$. Here $\mu_0 = 4\pi \times 10^{-7}$ H/m $\approx 1.257 \times 10^{-6}$ H/m is the magnetic constant, $\mu = 1$ is the magnetic permeability of vacuum. The masses M are subjected to the gravitational field with the constant $g \approx 9.8$ N/kg. The size of the magnet is assumed to be small compared to the length l . The Hamiltonian of this system is (we neglect frictional effects and the effect of the curvature of the chain)

$$H = \sum_n \mathcal{E}_n = \sum_n \left[\frac{p_n^2}{2M} + U(\theta_n, \theta_{n+1}) + V(\theta_n) \right], \quad (1)$$

where \mathcal{E}_n is the energy per the n th site, $p_n = Ml\dot{\theta}_n$ is the conjugate momentum and θ_n is the angle deviation from the equilibrium position of the n th pendulum (see Fig. 3), and the dot denotes the differentiation with respect to time t . Here the intersite potential U is given in terms of the

dipole-dipole interaction of adjacent magnets, i.e., $U(\theta_n, \theta_{n+1}) = D(\mathbf{m}_n, \mathbf{m}_{n+1}, r_n)$, where

$$r_n^2 = l^2 (\cos \theta_{n+1} - \cos \theta_n)^2 + [a + l(\sin \theta_{n+1} - \sin \theta_n)]^2 \quad (2)$$

is the distance between the n th and $(n+1)$ th magnets. The interaction between two magnetic dipoles \mathbf{m}_1 and \mathbf{m}_2 with a separation r is defined by

$$D(\mathbf{m}_1, \mathbf{m}_2, r) = \frac{1}{4\pi\mu_0} \left[\frac{(\mathbf{m}_1 \cdot \mathbf{m}_2) - 3(\mathbf{m}_1 \cdot \mathbf{n})(\mathbf{m}_2 \cdot \mathbf{n})}{r^3} \right]. \quad (3)$$

Here $\mathbf{n} = \mathbf{r}/r$ is the unit vector along the radius-vector \mathbf{r} which connects the magnets. The last term in the Hamiltonian (1) is the on-site potential for each pendulum resulting from its interaction with the gravitational field, so that $V(\theta) = Mgl(1 - \cos \theta)$.

Next, the dipole-dipole interaction can be rewritten in terms of the angles θ_n as follows:

$$U(\theta_n, \theta_{n+1}) = \frac{D_0 a^3 [\cos(\theta_{n+1} - \theta_n) - 3 \cos \alpha_n \cos \beta_n]}{r_n^3}, \quad (4)$$

where the constant D_0 is defined by $D_0 = D(\mathbf{m}_1, \mathbf{m}_2, a)|_{\theta_1=0, \theta_2=0} = m^2/4\pi\mu_0 a^3$, $m = |\mathbf{m}|$. The angles α_n and β_n are given in terms of θ_n and θ_{n+1} as

$$\cos \alpha_n = \frac{(\mathbf{m}_n \cdot \mathbf{n})}{m} = \frac{\sin \theta_n - \eta [1 - \cos(\theta_{n+1} - \theta_n)]}{r_n/a},$$

$$\cos \beta_n = \frac{(\mathbf{m}_{n+1} \cdot \mathbf{n})}{m} = \frac{\sin \theta_{n+1} + \eta [1 - \cos(\theta_{n+1} - \theta_n)]}{r_n/a}, \quad (5)$$

where $\eta = l/a$.

The soliton dynamics was observed experimentally in the circular chain consisting of 18 magnetic pendulums with $l = 0.118$ m. The magnitude of the dipole magnetic moment m cannot be measured directly, so the way to determine it is to measure the frequency of small-amplitude oscillations of a pendulum when its nearest neighbors are fixed. To this end, we consider the linearized version of equations of motion. Expanding all the terms in the Hamiltonian (1) up to the second order, we find

$$\ddot{\theta}_n = -(a_0 + g/l)\theta_n - a_1(\theta_{n-1} + \theta_{n+1}), \quad (6)$$

where $a_0 = 2(12\eta^2 - 1)D_0/MI^2$ and $a_1 = -2(1 + 6\eta^2)D_0/MI^2$. Then the linear dispersion law of small-amplitude waves $\theta_n(t) = \theta_0 \exp[i(nq - \omega t)]$ is given by

$$\omega^2 = \omega_0^2 - 2a_1(1 - \cos q), \quad \omega_0^2 = (Mgl - 6D_0)/MI^2, \quad (7)$$

where q is the wave number, $|q| \leq \pi$.

Consider now the oscillations of the n th pendulum in Eq. (6) when the $(n-1)$ th and $(n+1)$ th neighbors are fixed, i.e., $\theta_{n-1} = \theta_{n+1} = 0$. Then the frequency of these oscillations can easily be calculated and, as a result, we obtain

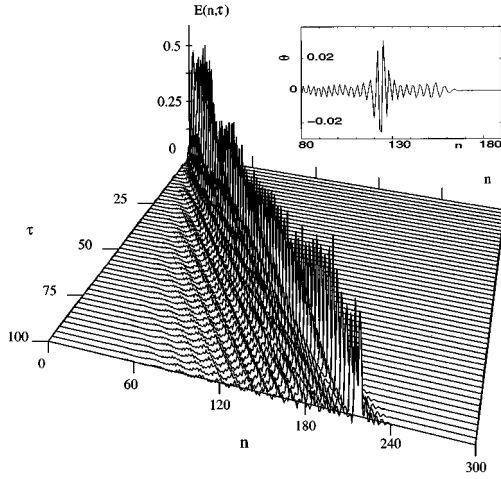


FIG. 4. The time evolution of the breather energy density $E(n, \tau)$ in the chain when only the second pendulum is disturbed: $\theta_2(0) = 0.1$, $\eta = 2.95$ ($a = 4.0$ cm). (Inset: amplitude of breather at $\tau = 20$.)

$$\omega^2 = \frac{g}{l} + \frac{12l^2 - a^2}{2\pi\mu_0 M l^2 a^5} m^2. \quad (8)$$

The magnitude of the dipole moment m was calculated from Eq. (8) by measuring the frequency ω . Thus, for the distance $a = 6.0$ cm the period of oscillations is $T = 0.587 \pm 0.001$ sec and therefore we found $m = 3.77 \times 10^{-7}$ HA m.

IV. NUMERICAL SIMULATIONS

We carried out numerical studies of the time evolution of the localized excitation in the chain of pendulums by using the standard fourth-order Runge-Kutta method to integrate the dynamical equations resulting from the Hamiltonian (1). In order to exhibit the breather uncluttered with radiation, we worked with a long chain with fixed boundary conditions. The numerical simulations of the formation and propagation of breather excitations have been carried out at the same initial conditions as in the experiments during the time of the order of 200 periods of breather oscillations. Initially the conditions were a deflection of the second pendulum (θ_2), and we observed the propagation of a narrow pulse with relatively permanent shape and velocity (see Fig. 4). The plot shows the time dependence of the dimensionless total energy $E(n, \tau) = \mathcal{E}_n(t)/D_0$ per the n th site against dimensionless time $\tau = \sqrt{D_0/M}l^2 t$. We varied the spacing a and calculated the breather velocity v . The results of these simulations are presented in Table I. The experimental and computational values of the velocity v are in reasonable agreement, considering the variability of the magnetic and mechanical proper-

TABLE I. The soliton velocities for different values of η .

$\theta_2(0)$	$\eta = l/a$	$\gamma = Mg l/D_0$	v , sites/sec	
			Experimental	Numerical
0.1	1.18	1100	1.75	2.01
	1.87	276	2.51	4.23
	2.95	71	4.83	5.20

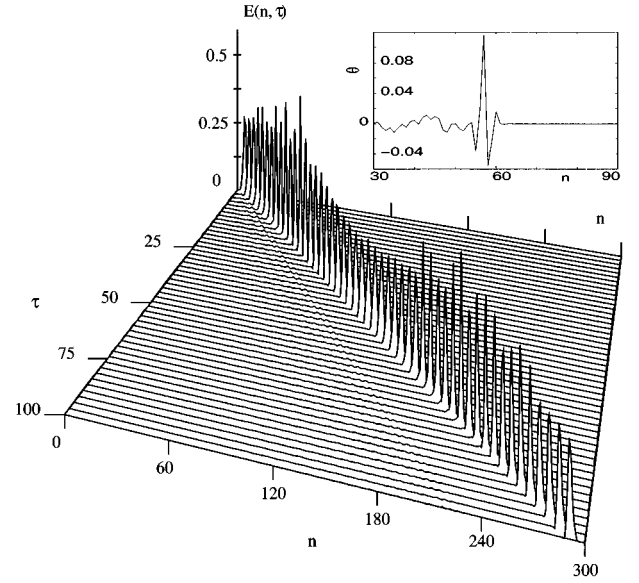


FIG. 5. The time evolution of the breather energy density $E(n, \tau)$ in the chain when only the second pendulum is disturbed: $\theta_2(0) = 0.25$, $\eta = 1.87$ ($a = 6.31$ cm). (Inset: amplitude of breather at $\tau = 20$.)

ties along the chain, the neglect of friction, and the approximation of dipole-dipole interactions when the separation lengths are comparable with the size of the magnets. With a larger initial deflection in the numerical simulation, we obtained a cleaner breather profile, as shown in Fig. 5.

V. A CONNECTION WITH AN INTEGRABLE DISCRETE MODEL

Now we consider some analytical approximations which enable us to make contact with an integrable discrete model, the Ablowitz-Ladik model.¹³ To study large-amplitude waves we need to keep nonlinear terms in the Hamiltonian (1). First, we can expand all the expressions in the Hamiltonian (1) up to the fourth order. As a result, after lengthy but straightforward calculations we obtain a truncated version of the Hamiltonian (1) and derive the following equations of motion:

$$\begin{aligned} \ddot{\theta}_n + (a_0 + g/l)\theta_n + a_1(\theta_{n-1} + \theta_{n+1}) + b_1[\theta_n(\theta_{n-1} - \theta_{n+1}) \\ + (\theta_{n+1}^2 - \theta_{n-1}^2)/2] + (c_0 - g/6l)\theta_n^3 + c_1[\theta_n^2(\theta_{n-1} \\ + \theta_{n+1}) + (\theta_{n-1}^3 + \theta_{n+1}^3)/3] + c_2\theta_n(\theta_{n-1}^2 + \theta_{n+1}^2) \approx 0, \end{aligned} \quad (9)$$

where a_0 and a_1 have been defined above while the remaining coefficients are $b_1 = 12\eta(1 + 5\eta^2)D_0/Ml^2$, $c_0 = (1/3 - 97\eta^2 + 120\eta^4)D_0/Ml^2$, $c_1 = (1 - 12\eta^2 - 180\eta^4) \times D_0/Ml^2$, and $c_2 = (1/2 + 129\eta^2/2 + 180\eta^4)D_0/Ml^2$. We use the rotating wave approximation¹⁴ and look for solutions to Eq. (9) in the form $\theta_n(t) = \phi_n(t)\exp(-i\omega_0 t) + \text{c.c.}$, where $\phi_n(t)$ is the complex amplitude of large-amplitude pendulum oscillations. Applying this approximation, i.e., keeping in Eq. (9) only terms with $\exp(-i\omega_0 t)$, and assuming that $|\dot{\phi}_n(t)| \ll \omega_0 |\phi_n|$, Eq. (9) can be reduced to a perturbed version of the Ablowitz-Ladik equation. The coefficients of this

equation depend on the perturbative terms we choose. We fit them in such a way that the perturbative terms are negligible. Thus, if the amplitudes $\phi_n(t)$'s vary smoothly from site to site in the chain, then omitting the perturbative terms, the Ablowitz-Ladik equation takes the following approximate form:

$$i\dot{\phi}_n + \sigma(\phi_{n+1} - 2\phi_n + \phi_{n-1}) + \frac{\lambda}{2}|\phi_n|^2(\phi_{n-1} + \phi_{n+1}) = 0, \quad (10)$$

with the coefficients $\sigma = -a_1/2\omega_0$ and $\lambda = (Mgl - 24D_0)/8Ml^2\omega_0$. These explicit values were the main goal of the analytical calculations. Having them, one can easily write the resulting approximate breather solution of Eq. (9) for large-amplitude pendulum oscillations

$$\theta_n(t) \approx \theta_0 \operatorname{sech}\left(\frac{n-vt}{L}\right) \cos(nq - \omega t). \quad (11)$$

Note, that the amplitude θ_0 and wave number q are arbitrary parameters. Here θ_0 and the breather width L are related by

$$\frac{1}{L} = \ln \left[\theta_0 \sqrt{\frac{2\lambda}{\sigma}} + \sqrt{\frac{2\theta_0^2\lambda}{\sigma} + 1} \right]. \quad (12)$$

The group (breather) velocity v and the carrier frequency ω are given by

$$v = 2\sigma L \sinh(1/L) \sin q, \\ \omega = \omega_0 + 2\sigma [1 - \cosh(1/L) \cos q]. \quad (13)$$

At least, in the continuum limit ($L \gg a$) the approximate solution of Eq. (9) given by Eqs. (11)–(13) is valid. However, we have also checked this approximation numerically in the case of narrower solutions when L/a is small. To this end, we used Eqs. (11)–(13) as initial condition for simulations of the equations of motion. As a result, we obtained stable breathers propagating with constant shape and velocity, and again there was a good correspondence with the experiments. In this approximation we obtained a clear breather solution which separates itself from the parasitic oscillations, as one can see from the plot of the energy distribution $E(n, \tau)$ in Fig. 6.

VI. CONCLUSION

In this paper we have presented a nonlinear model which seems to be the first experimental example which visually

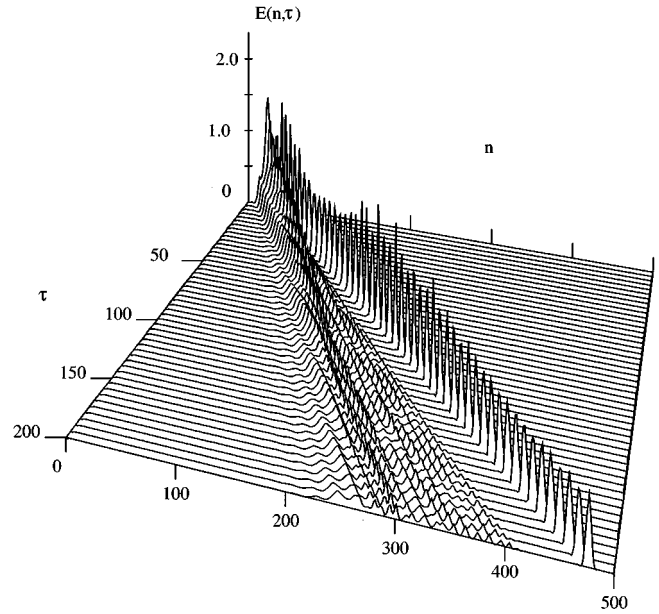


FIG. 6. The time evolution of the breather energy density $E(n, \tau)$ in the chain with the Ablowitz-Ladik initial conditions (11)–(13): $\theta_0 = 0.1$, $\eta = 1.87$ ($a = 6.31$ cm), $q = 1.5$.

demonstrates stable moving breathers (envelope solitons) in anharmonic lattices with in-line on-site potentials. This type of nonlinear excitations is different from the well-known supersonic Toda-like solitons which describe the propagation of a lattice deformation of a constant profile. Finally, we wish to point out that the mechanism of moving breathers should be important in various physical¹⁵ and industrial processes since it allows the transport of vibrational energy over long distances by nondiffusional mechanisms. The model has interest in its own right as a pedagogical tool in the study of nonlinear lattices.

ACKNOWLEDGMENTS

We are grateful to S. Flach for several helpful conversations. This work was supported by the British Council Alliance project. One of us (Y.Z.) wishes to acknowledge the financial support of Heriot-Watt University.

¹R. S. MacKay and S. Aubry, *Nonlinearity* **7**, 1623 (1994).

²S. Flach, *Phys. Rev. E* **51**, 3579 (1995), and references therein.

³A. J. Sievers and S. Takeno, *Phys. Rev. Lett.* **61**, 970 (1988).

⁴Yu. S. Kivshar, *Phys. Lett. A* **161**, 80 (1991).

⁵T. Dauxois, M. Peyrard, and C. R. Willis, *Physica D* **57**, 267 (1992).

⁶T. Dauxois and M. Peyrard, *Phys. Rev. Lett.* **70**, 3935 (1993).

⁷O. Bang and M. Peyrard, *Phys. Rev. E* **53**, 4143 (1996).

⁸A. C. Scott, *Am. J. Phys* **37**, 52 (1969). Breathers can easily be generated in the mechanical SG model but details were never

published [A. C. Scott (private communication)].

⁹F. M. Russell and D. R. Collins, *Radiat. Meas.* **25**, 67 (1995).

¹⁰F. M. Russell and J. W. Steeds, *Nucl. Tracks Radiat. Meas.* **22**, 65 (1993).

¹¹R. H. Silbee, *J. Appl. Phys.* **28**, 1246 (1957).

¹²F. M. Russell and D. R. Collins, *Nucl. Instrum. Methods Phys. Res. B* **105**, 30 (1995).

¹³M. J. Ablowitz and J. F. Ladik, *Stud. Appl. Math.* **55**, 213 (1976).

¹⁴For details see, e.g., C. Claude, Yu. S. Kivshar, K. H. Spatckek, and O. Kluth, *Phys. Rev. B* **47**, 14 228 (1993).

¹⁵F. M. Russell and D. R. Collins, *Phys. Lett. A* **216**, 197 (1996).